

Energy distribution for waves in transcritical flows over a bump

Samual Shan-Pu Shen *

Department of Mathematics, University of Alberta, Edmonton, Canada T6G 2G1

Received 4 April 1993; revised 21 June 1995

Abstract

Undisturbed water in a two-dimensional long channel obtains mechanical energy from a moving bump on the bottom of the channel. When the bump moves to the left at a speed near the critical shallow water wave velocity $(gH)^{1/2}$, the free surface of the water consists of a soliton zone upstream, and a uniform depression zone and a wake zone downstream. Lee, Yates and Wu [J. Fluid Mech. 199, 569–593 (1989)] computed the drag on the bump and the total energy of the water waves. In this paper, we answer the question how the total energy is distributed among the zones of the upstream solitons, the downstream depression and the downstream wakes. From the energy distribution formulas derived in Section 3, we conclude that: (i) The energy of the downstream wake is a decreasing function of the Froude number F and contains almost all the energy when F is small but still in the transcritical range; (ii) the soliton energy is an increasing function of F and contains most energy of the system when F is large but still in the transcritical range; (iii) the depression energy does not vary significantly with F ; (iv) the soliton energy is smaller (greater) than the depression energy when the Froude number is small (large respectively); and (v) the wake energy is greater (smaller) than the depression energy when the Froude number is small (large respectively). Hence our results analytically show that the drag on a vessel moving at a transcritical speed is mainly due to the waves ahead of the vessel when its cruising speed is large and the waves behind the vessel when its speed is low. These conclusions agree with the pertinent concepts of moving vessel designs.

1. Introduction

Ref. [1] considered the water over a bump on the flat bottom of a two-dimensional open channel of infinite length. The water is assumed to be an inviscid and incompressible fluid with constant density. The height of the bump is less than half the water depth at infinity. Initially, the water is at rest and the free surface is hence flat. Mechanical energy is supplied to the water by towing the bump toward left (upstream) at a speed near the shallow wave velocity $(gH)^{1/2}$, where H is the depth of the fluid at infinity and g the gravitational acceleration. The water is thus disturbed by the moving bump. The work done by the bump to the water accounts for the mechanical energy of the wave motion of the disturbed water.

When the bump velocity is near the shallow water wave speed $(gH)^{1/2}$, the water motion can never approach a stationary state and this intrinsically unsteady state is called the transcritical state. At the transcritical state,

* E-mail shen@cake.math.ualberta.ca.

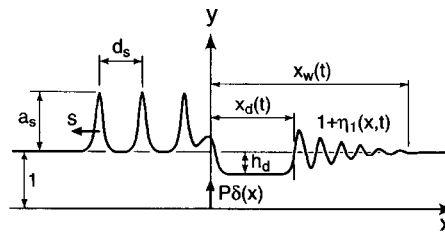


Fig. 1. An illustration of the solution $\eta_1(x, t)$ of the fKdV Eq. (1) for a fixed time t . The coordinate frame is in the dimensionless variables. The dimensionless free surface profile is $1 + \epsilon\eta_1(x, t)$ rather than $1 + \eta_1(x, t)$ shown here.

experiments, numerical simulations and asymptotic analyses all indicate the existence of a train of solitons of equal size moving upstream ahead of the bump [1–3]. Immediately behind the bump there is a flat depression zone behind which there is a wake zone (see Fig. 1). As time increases, the number of upstream advancing solitons increases at a constant rate. The depth of the depression remains the same but the length of the depression zone increases (the right-hand end of the depression zone moves to the right at a constant speed while the left-hand end remains fixed at the site of the forcing). The length of the wake zone behind the depression also increases since the right-hand end of the wake zone moves to the right faster than its left-hand end which is the right-hand end of the depression zone.

Ref. [1] calculated the total drag on the bump and hence the total work done by the bump to the water motion. When neglecting friction and viscous dissipation, the resulting mechanical energy of the water motion is equal to the total work. An interesting question is how this total energy is distributed in the aforementioned three zones of wave motion: the upstream soliton zone, the downstream depression zone and the downstream wake zone. An answer to this question will show how much contribution each wave zone makes to the drag on the bump. Hence, this answer is very important in floating vessel designs. The main purpose of this paper is to provide such an answer.

It appears that it is difficult, if not impossible, to measure the drag on the bump caused by each wave zone separately in a laboratory. It is also difficult to calculate the drag by numerically solving the Euler equations. It seems that the best alternative to quantitatively estimate the drag caused by each wave zone is by asymptotic analysis. Both Refs. [1] and [4] show that forced Korteweg–de Vries equation (fKdV) is an accurate model when the bump's height is in comparable scale to its length. In this case, Ref. [4] further shows that the bump forcing in the fKdV can be represented by a Dirac delta function. Ref. [6] (p. 87, before Eq. (38)) postulated that the mass of the upstream solitons solely comes from the downstream depression and the mass of the downstream wake is almost zero. Our numerical tests show that this mass postulate is accurate (with less than 2% relative error) when the Froude number is near unity. With this postulate, one can find approximate formulas for the depth of the downstream depression, the amplitude and the period of the upstream solitons as functions of the bump velocity and the bump area. This was done in Refs. [1,3,6]. Ref. [1] showed that these formulas are very accurate when the Froude number is near unity. To make the paper self-contained, relevant derivations of these formulas will be recapitulated at suitable places. The new in this paper are the calculations of the energy of each wave zone and the drag caused by each wave zone. Our conclusions are: (i) The energy of the downstream wake is a decreasing function of the Froude number F and contains almost all the energy when F is small but still in the transcritical range; (ii) the soliton energy is an increasing function of F and contains most energy of the system when F is large but still in the transcritical range; (iii) the depression energy does not vary significantly with F ; (iv) the soliton energy is smaller (greater) than the depression energy when the Froude number is small (large respectively); and (v) the wake energy is greater (smaller) than the depression energy when the Froude number is small (large respectively). Hence our results analytically show that the drag on a vessel moving at a transcritical speed is mainly due to the waves ahead of the vessel when its cruising speed is large and the waves behind the vessel when its speed is low. These conclusions agree

with the pertinent concepts of moving vessel designs. To my knowledge, these conclusions have not been made in previous studies on the fKdV.

Let W , E_s , E_d and E_w denote respectively the total work done to the water by the bump, the mechanical energy of the soliton zone, the depression zone and the wake zone. Thus, $W = E_s + E_d + E_w$. Therefore, the aim of this paper is to find the functions which describe the dependence of W , E_s , E_d and E_w on the bump area $S = \int_{x_-}^{x_+} h^*(x^*) dx^*$ and the bump velocity $c^* = (gH)^{1/2}(1 + \epsilon\lambda)$, where the asterisk “*” signifies the dimensional quantity. The Froude number is hence $F = 1 + \epsilon\lambda$.

In Section 2, we derive the expression for the total mechanical energy. In Section 3, the total work done to the water by the bump and the energy of solitons, the depression and the wakes are expressed in terms of c^* and S . Conclusions and discussions are given in Section 4.

2. The total mechanical energy of the wave motion

The reference frame (x^*, y^*) is fixed on the bump. It is assumed that the bump is small and described by $h^*(x^*) = \epsilon^2 H h(x)$, where the small parameter ϵ is defined by $\epsilon = (H/L)^2 \ll 1$ and computed by $(\|h\|_\infty/H)^{1/2}$. Here $\|h\|_\infty$ is the maximum height of the bump, and the quantity L is the horizontal length scale. Hence $x^* = xL$. The free surface is assumed to be $\eta^* = \epsilon H \eta_1(x, t) + O(\epsilon^2)$. When $c^* = (gH)^{1/2}(1 + \epsilon\lambda)$, the function $\eta_1(x, t)$ satisfies a forced Korteweg–de Vries equation (fKdV) [1–4]:

$$\eta_{1t} + \lambda \eta_{1x} - \frac{3}{2} \eta_1 \eta_{1x} - \frac{1}{6} \eta_{1xxx} = \frac{h_x(x)}{2}, \quad -\infty < x < \infty. \tag{1}$$

When considering a stationary solution, the forcing function $h(x)$ can be approximated by $P\delta(x)$ and $P = \epsilon^{-3/2} S/H^2$ is the dimensionless area of the bump and $\delta(x)$ is the Dirac delta function. The delta function approximation for a bump whose base length is comparable to its height has been addressed in Ref. [4]. The solution to an initial value problem for the fKdV gives an approximation to the free surface profile by $\eta^* \approx \epsilon H \eta_1(x, t)$. Meantime, the approximate velocity and pressure fields are

$$(u^*, v^*) \approx (-\epsilon \eta_1, \epsilon^{3/2} \eta_{1xy})(gH)^{1/2}, \quad p^* = \rho g[-(1 - y^*/H) + \epsilon \eta_1].$$

A schematic solution of Eq. (1) is shown in Fig. 1. Refs. [1,2,4] show that the above fKdV (1) is a very good model for the flows under investigation, even when the values of ϵ are relatively large, say, $\epsilon = 0.5$ or $\|h\|_\infty = H/4$.

We are concerned exclusively with the initial condition $\eta^*(x^*, t^* = 0) = 0$. The mass conservation property of the wave motion gives the following identity

$$\int_{-\infty}^{\infty} \rho \eta^*(x^*, t^*) dx^* = 0 \tag{2}$$

for every $t^* \geq 0$. Here, the dimension for the density ρ is [mass][area]⁻¹.

The horizontal momentum M_h of the perturbed flow due to the bump motion is

$$\begin{aligned} M_h &= \int_{-\infty}^{\infty} dx^* \int_{h^*}^{H+\eta^*} dy^* \rho u^*(x^*, y^*, t^*) \\ &= \int_{-\infty}^{\infty} d(\epsilon^{-1/2} Hx) \int_{\epsilon^2 Hh}^{H(1+\epsilon\eta_1)} d(Hy) \left[\rho \epsilon \left(-\eta_1(x, t)(gH)^{1/2} \right) \right] + \rho H^2 (gH)^{1/2} O(\epsilon^{5/2}). \end{aligned}$$

The above yields

$$M_h = -\epsilon^{3/2} \rho H^2 (gH)^{1/2} \int_{-\infty}^{\infty} \eta_1^2(x, t) dx + \rho H^2 (gH)^{1/2} O(\epsilon^{5/2}). \quad (3)$$

The negative sign “–” implies that the horizontal momentum is oriented toward upstream because the impulse exerted by the bump to the water is toward the upstream direction.

Similarly, it can be shown that the vertical momentum M_v is of order $\epsilon^5 \rho H^2 (gH)^{1/2}$, which is negligible in relation to M_h .

The total mechanical energy E of the perturbed flow is equal to the sum of the kinetic energy E_k and the potential energy E_p . Here we take the potential with respect to half the depth of the rest water. Hence we have

$$\begin{aligned} E &= \int_{-\infty}^{\infty} dx^* \int_{h^*}^{H+\eta^*} dy^* \left[\frac{\rho}{2} \left((u^*(x^*, y^*, t^*))^2 + (v^*(x^*, y^*, t^*))^2 \right) + \rho g \left(y^* - \frac{H+h^*}{2} \right) \right] \\ &= \int_{-\infty}^{\infty} d(\epsilon^{-1/2} Hx) \int_{\epsilon^2 Hh}^{H(1+\epsilon\eta)} d(Hy) \left\{ \frac{\rho}{2} \left[\left(\epsilon(-\eta_1(x, y, t))(gH)^{1/2} \right)^2 + \left(\epsilon^{1/2} (gH)^{1/2} \epsilon \eta_{1,x} y \right)^2 \right] \right. \\ &\quad \left. + \rho g H \left(y - \frac{1}{2} (1 + \epsilon^2 h) \right) \right\} + \rho g H^3 O(\epsilon^{7/2}). \end{aligned}$$

The above yields

$$E = -(gH)^{1/2} M_h + \frac{\rho g H^3}{2} \epsilon^{5/2} \int_{-\infty}^{\infty} \left[\eta_1^3 + \frac{1}{3} \eta_{1,x}^2 - \eta_1 h \right] dx + \rho g H^3 O(\epsilon^{7/2}). \quad (4)$$

3. Energy distribution

The k th upstream soliton solution of the fKdV (1) may be expressed in the following form

$$\eta_1^{(k)}(x, t) = 2(\lambda + s) \operatorname{sech}^2 \left\{ \left[(3/2)(\lambda + s) \right]^{1/2} (x + st - x_k) \right\}, \quad (5)$$

where s is the upstream advancing speed of the soliton, $a_s = 2(\lambda + s)$ is the amplitude of the soliton, and x_k is the phase shift. For each soliton $\eta_1^{(k)}$, one has

$$\begin{aligned} \int_{-\infty}^{\infty} (\eta_1^{(k)})^2 dx &= 8 \left(\frac{2}{3} (\lambda + s) \right)^{3/2} = 8 \left(\frac{a_s}{3} \right)^{3/2}, \\ \int_{-\infty}^{\infty} \left[(\eta_1^{(k)})^3 + \frac{1}{3} \eta_{1,x}^{(k)2} \right] dx &= \frac{32}{3} (\lambda + s)^{5/2} = \frac{4\sqrt{2}}{3} a_s^{5/2}. \end{aligned}$$

Let $N_s(t)$ be the total number of mature solitons upstream at a large time t . Then the mechanical energy of the upstream solitons is

$$E_s = \rho g H^3 \epsilon^{3/2} N_s(t) 8 \left(\frac{a_s}{3} \right)^{3/2} + \rho g H^3 \epsilon^{5/2} N_s(t) \frac{2\sqrt{2}}{3} a_s^{5/2}. \quad (6)$$

The first term is $-M_{hs}\sqrt{gH}$ and

$$M_{hs} = -\rho g H^2 \sqrt{gH} \epsilon^{3/2} N_s(t) \int_{-\infty}^{\infty} (\eta_1^{(k)})^2 dx = -\rho g H^2 \sqrt{gH} \epsilon^{3/2} N_s(t) 8 \left(\frac{a_s}{3}\right)^{5/2}. \quad (7)$$

is the total horizontal momentum of the all upstream solitons.

To find the mechanical energy of the downstream depression, we evaluate

$$\int_0^{x_d} \left(\eta_1^3 + \frac{1}{3}\eta_{1x}^2\right) dx = -h_d^3 x_d. \quad (8)$$

where $h_d \geq 0$ is the depth of the depression and $x_d \geq 0$ is the length of the depression zone. The depression depth h_d may be determined by the mass postulate that the soliton mass comes solely from the depression (See Ref. [6], p. 87, before Eq. (38)). The average height of the upstream is h_s , that is, the average of $\eta_1(x, t)$ with respect x over a period d_s , the distance between the two peaks of any two adjacent solitons. When time is large, we regard h_s as an upstream uniform state which falls to the downstream uniform state h_d . Both of these uniform states extend to infinity as time $t \rightarrow \infty$ and form an “imaginary” stationary state $v(x)$. This stationary state is governed by the following boundary value problem:

$$\lambda v_x - \frac{3}{2} v v_x - \frac{1}{6} v_{xxx} = \frac{P}{2} \delta_x(x), \quad -\infty < x < \infty, \quad (9)$$

$$v(-\infty) = h_s \quad \text{and} \quad v(\infty) = -h_d. \quad (10)$$

Let $v(x) = \zeta(x) + h_s$. Then the above two equations become the hydraulic fall type of boundary value problem for $\zeta(x)$ [4,5]:

$$\left(\lambda - \frac{3}{2}h_s\right)\zeta_x - \frac{3}{2}\zeta\zeta_x - \frac{1}{6}\zeta_{xxx} = \frac{P}{2}\delta_x, \quad \zeta(-\infty) = 0, \quad \zeta(\infty) = -(h_s + h_d).$$

This boundary value problem is solvable only when $\zeta(x)$ is a smooth fall from the upstream zero solution to a downstream solitary wave tail (see Eqs. (33)–(44) in Ref. [5]). Hence $\lambda - \frac{3}{2}h_s < 0$ and $\zeta(x) = 0$ for all x in $(-\infty, 0)$. The first integral of the above boundary value problem in $(0, \infty)$ results in

$$\left(\lambda - \frac{3}{2}h_s\right)\zeta - \frac{3}{4}\zeta^2 - \frac{1}{6}\zeta_{xx} = 0 \quad \text{when } x > 0, \\ \zeta(0+) = 0, \quad \zeta_x(0+) = -3P, \quad \zeta(\infty) = -(h_s + h_d).$$

Another first integral of this boundary value problem results in

$$\frac{1}{3}\zeta_x^2 = -\zeta^3 + 2\left(\lambda - \frac{3}{2}h_s\right)\zeta^2 + 3P^3 \quad \text{when } x > 0, \\ \zeta(\infty) = -(h_s + h_d).$$

This problem is solvable only when the third order polynomial on the right hand of the differential equation has a double zero. This double zero condition is

$$h_s = \left(\frac{3}{4}P^2\right)^{1/3} + \frac{2}{3}\lambda. \quad (11)$$

The amplitude of the fall of the downstream solitary wave tail is

$$-\frac{4}{3}\left(\lambda - \frac{3}{2}h_s\right),$$

which has to be equal to $h_s + h_d$. This leads to the important formula for h_d

$$h_d = \left(\frac{3}{4}P^2\right)^{1/3} - \frac{2}{3}\lambda. \quad (12)$$

This formula is the same as formula (4.30a) given in Ref. [3] with different coefficients. It shows that the depression depth h_d is a linear function of λ . This conclusion agrees with the numerical results in Ref. [1] (see the β -curve in Fig. 9 of Ref. [1]).

The quantity x_d can be determined by the same mass postulate used above that leads to

$$N_s m_s = x_d h_d \quad (13)$$

where $m_s = 4[(2/3)(\lambda + s)]^{1/2} = 4(a_s/3)^{1/2}$ is the mass of an upstream soliton.

Eqs. (4) and (8) together with the above equation lead to

$$E_d = \epsilon^{3/2} \rho g H^3 N_s 4 h_d \left(\frac{a_s}{3}\right)^{1/2} - \rho g H^3 \epsilon^{5/2} N_s 4 (a_s/3)^{1/2} h_d^2. \quad (14)$$

Here the first term is equal to $-M_{hd}\sqrt{gH}$ and

$$M_{hd} = -\epsilon^{3/2} \rho H^2 \sqrt{gH} N_s 4 h_d \left(\frac{a_s}{3}\right)^{1/2}. \quad (15)$$

is the momentum of the depression zone. Again, the negative sign for this quantity means that the impulse exerted to the flow by the bump is toward to the upstream direction.

It seems not easy to find the wake energy E_w directly. So we evaluate the total work W done to the water by the bump. Then the wake energy E_w can be found as $W - E_s - E_d$.

Let x_D be any point in the depression zone. The long time average of the operation $\int_{-\infty}^{x_D} (1) \times \eta_1(x, t) dx$ yields

$$\frac{M_{hs}^{(1)}}{T_s} = -\lambda h_d^2 - h_d^3 + C_w, \quad \text{where} \quad C_w = \int_{-\infty}^{x_D} \eta_1(x, t) h_x(x) dx$$

is the drag coefficient. Making use of formulas (11), (12) and (35) in the Appendix, the total drag on the bump is $D_w^* = C_w \rho g H^2$ and is equal to

$$D_w^* = \frac{3}{2} \rho g H^2 \epsilon^{3/2} P^2. \quad (16)$$

In the following, we need other formulas derived in [1]. They are

$$a_s = 2(h_d + \frac{4}{3}\lambda)(h_d + \frac{1}{3}\lambda)/h_d, \quad (17)$$

$$T_s = \frac{16}{3} \left[\frac{2(h_d + \frac{1}{3}\lambda)}{3h_d^3(h_d + \frac{4}{3}\lambda)} \right]^{1/2}. \quad (18)$$

In order to make the paper self-contained, in the appendix we include another derivation of the above two formulas which follows the same line as that given in Ref. [1]. Numerical tests show that these two formulas are very accurate when $|\lambda|$ is small.

The total work done by the bump up to the time $N_s T_s (H/g)^{1/2}$ when N_s solitons are mature is

$$W = D_w^* N_s T_s (H/g)^{1/2} (1 + \epsilon \lambda) (gH)^{1/2}.$$

This yields

$$W = \frac{3}{2} N_s \rho g H^3 \epsilon^{3/2} P^2 T_s (1 + \epsilon \lambda). \quad (19)$$

From Eqs. (7), (15), (19), (6), and (14), we can obtain the following energy distribution results:

$$E_s = N_s \rho g H^{1/2} \frac{2}{9} a_s^{*3/2} (4\sqrt{3}H + 3\sqrt{2}a_s^*), \quad (20)$$

$$E_d = N_s \rho g H^{1/2} \frac{2\sqrt{3}}{3} h_d^* a_s^{*1/2} (2H - h_d^*), \quad (21)$$

$$W = \frac{3}{2} N_s \rho g H^{-2} \epsilon^{-3/2} S^2 T_s^* c^*, \quad (22)$$

where $T_s^* = \epsilon^{-3/2} T_s (H/g)^{1/2}$ is the dimensional soliton generation period, $h_d^* = \epsilon H h_d$ the dimensional depth of the depression, $a_s^* = \epsilon H a_s$ the dimensional amplitude of the solitons, and $S = \epsilon^{3/2} H^2 P$ as defined after Eq. (1) is the area of the bump. The above energy expressions can be normalized by the energy dimension $\rho g H^3$ and further by the number of solitons N_s . The expressions for the dimensionless energy per soliton are:

$$e_s = \frac{E_s}{N_s \rho g H^3} = \frac{2}{9} \epsilon^{3/2} a_s^{*3/2} (4\sqrt{3} + 3\sqrt{2}\epsilon a_s), \quad (23)$$

$$e_d = \frac{E_d}{N_s \rho g H^3} = \frac{2\sqrt{3}}{3} \epsilon^{3/2} h_d^* a_s^{*1/2} (2 - \epsilon h_d), \quad (24)$$

$$w = \frac{W}{N_s \rho g H^3} = \frac{3}{2} \epsilon^{3/2} P^2 T_s (1 + \epsilon \lambda), \quad (25)$$

$$e_w = \frac{W - E_s - E_d}{N_s \rho g H^3} = w - e_s - e_d. \quad (26)$$

Over a long time, the energy on the short zone over the bump is negligible in comparison with e_s and e_d . Hence we have equality (26).

In Ref. [5], the transcritical range has been found to be (λ_L, λ_C) with $\lambda_L = -(3/4)(6P^2)^{1/3}$ and $\lambda_C = (3/4)(3P^2/2)^{1/3}$. If $\lambda = \lambda_L$, then $h_d + (4/3)\lambda = 0$. Hence $T_s \rightarrow \infty$ as $\lambda \rightarrow \lambda_L + 0$ by Eq. (18). Consequently, it takes infinitely long time for a soliton to mature and to be radiated upstream. Therefore, the mass postulate becomes invalid and formulas (17) and (18) become inaccurate when λ is near λ_L . Numerical results in Ref. [1] agree with this conclusion.

Despite that W takes a finite value when $\lambda = \lambda_C$, the above energy distribution formulas again become invalid at $\lambda = \lambda_C$. The reason is that at λ_C , the wake energy e_w is negative if it is calculated according to Eq. (26). The soliton energy is an increasing function of λ and the increasing rate becomes larger and larger when λ approaches λ_C from below. From formula (26) it happens that $e_w = 0$ when $\lambda = \lambda_0 < \lambda_C$. Hence e_w calculated from Eq. (26) is negative when $\lambda_0 < \lambda \leq \lambda_C$. For example, in the case of semi-circular bumps $R = 0.1H$ and $0.25H$, the corresponding values of the Froude number $F_0 = 1 + \epsilon \lambda_0$ are 1.02407 and 1.02410, respectively. Therefore, the largest interval in which the derived energy distribution formulas are valid is $(1 + \epsilon \lambda_L)(gH)^{1/2} < c^* < (1 + \epsilon \lambda_0)(gH)^{1/2}$. In this interval, E_s, E_d and W are smooth functions of λ for a given P . The energy distribution formulas have been plotted against the Froude number $F = 1 + \epsilon \lambda$ in Figs. 2a and 2b for two semi-circular bumps $R = 0.1H$ and $0.25H$, where R is the radius of a semi-circular bump. In these figures, $\epsilon = (R/H)^{1/2}$ and $P = (\pi/2)\epsilon^{3/2}$. When $R/H = 0.1, 0.25$, the transcritical range

$$(F_L, F_C) = (1 + \epsilon \lambda_L, 1 + \epsilon \lambda_C) = (1 - (1/2)(9S/(2H^2))^{2/3}, 1 + (1/2)(9S/(4H^2))^{2/3})$$

for the Froude number F is (0.9146, 1.0539) and (0.7100, 1.1827), respectively. The energy formulas are plotted in subintervals of the above transcritical ranges: (0.9146, 1.02407) for $R = 0.1H$ and (0.7100, 1.02410) for $R = 0.25H$. These plots show how the quantities w, e_s, e_d and e_w vary with the Froude number F for a fixed

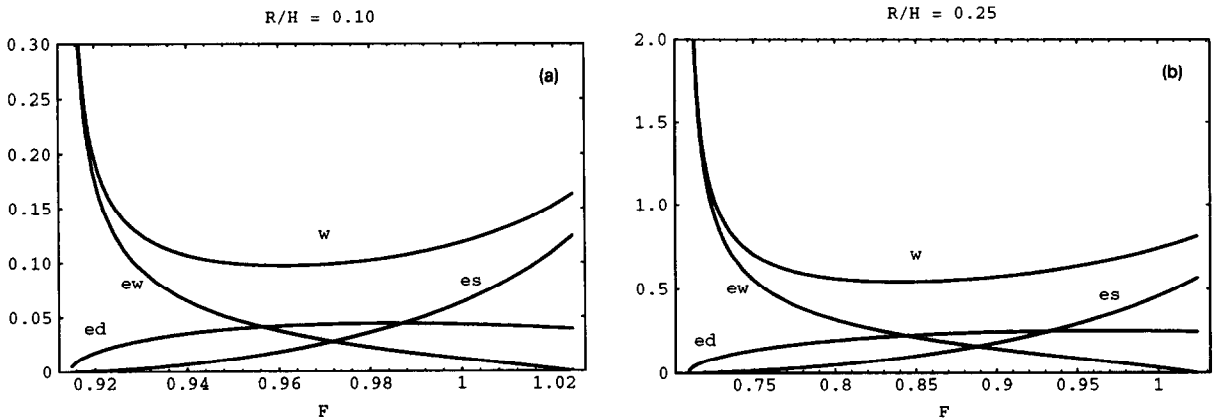


Fig. 2. The relationships e_s , e_d , e_w and w vs. F . Here, $F = 1 + \epsilon\lambda$ is the Froude number, $\epsilon = (R/H)^{1/2}$ the small number for the asymptotic analysis and R the radius of the semi-circular bump: (a) $R/H = 0.1$ in the interval $(F_L, F_0) = (0.91460, 1.02407)$, and (b) $R/H = 0.25$ in the interval $(F_L, F_0) = (0.71000, 1.02410)$.

forcing. From Fig. 2b, we notice that the e_s curve has a sharp turning point around $F = 0.72$. When $F < 0.72$, e_s and e_d almost vanish while e_w absorbs almost all the external energy which is supplied to the water by the bump. The energy accumulated by the downstream wake is now infinite relative to the energy of an upstream soliton. The phenomenon is the manifestation that the downstream wake becomes dominant. This explanation is supported by Fig. 2a in [1].

Again from Fig. 2b, we notice that when F is close to 1.024, for each upstream soliton produced one needs to supply almost no energy to the wake zone and hence the wake zone is relatively short. This is supported by Fig. 2c in Ref. [1].

4. Conclusions and discussions

Based upon the approximation that the upstream soliton mass comes solely from the downstream depression, we have analytically found the mechanical energy distribution of transcritical water wave motion over a bump. For a fixed bump area, the wake energy per soliton is a decreasing function of the Froude number F while a single soliton energy is an increasing function of F . In the transcritical range (F_L, F_C) of the Froude number F , when F is approaching F_L from the right, the downstream wake energy e_w per soliton becomes infinite according to formula (26) and the wake absorbs almost all the input energy W . When F is approaching F_0 from the left, the upstream soliton zone contains more energy than that of the wake zone and that of the depression zone.

The energy of the depression zone does not vary significantly with the Froude number F . The soliton energy is smaller (greater) than the depression energy when the Froude number is small (large, respectively). The wake energy is greater (smaller) than the depression energy when the Froude number is small (large, respectively). Hence, the drag on a vessel moving at a transcritical speed is mainly due to the waves ahead of the vessel when its cruising speed is large and the waves behind the vessel when its speed is low. These conclusions agree with the pertinent concepts of moving vessel designs.

The long time average of the total drag $D_w^* = (3/2)\epsilon^{3/2}P^2\rho gH^2$ does not vary with the Froude number. This conclusion is supported by Fig. 6 in Ref. [1] when $0.8 < F < 1.05$. It is clear to us that the drag is caused by waves. The contributions to the total drag from the upstream soliton zone, downstream depression zone and downstream wake zone can be described respectively by the following formulas

$$D_{ws}^* = \frac{e_s}{T_s(1 + \epsilon\lambda)} \rho g H^2 = \epsilon^{3/2} \frac{2}{3} a_s^{3/2} (4\sqrt{3} + 3\sqrt{2}\epsilon a_s) \rho g H^2,$$

$$D_{wd}^* = \frac{e_d}{T_s(1 + \epsilon\lambda)} \rho g H^2 = \frac{E_d}{N_s \rho g H^3} = \frac{2\sqrt{3}}{3} \epsilon^{3/2} h_d a_s^{1/2} (2 - \epsilon h_d) \rho g H^2,$$

$$D_{ww}^* = \frac{w - e_s - e_d}{T_s(1 + \epsilon\lambda)} \rho g H^2.$$

Whether it is possible to reduce the upstream radiated waves at a larger transcritical speed and suppress the downstream wake at the lower transcritical speed is an interesting question for optimal shape designs of moving vessels.

Appendix. Derivation of formulas (17) and (18)

Now, it is appropriate for us to estimate the soliton amplitude a_s and the soliton generation period T_s . The following two first integrals are obtained by doing $\int_{-\infty}^{0-} (1) dx$ and $\int_{-\infty}^{0-} \eta_1(x, t) \times (1) dx$

$$\frac{m_s}{T_s} = -\lambda \eta_1(0, t) + \frac{3}{4} \eta_1^2(0, t), \quad (27)$$

$$\frac{M_{hs}^{(1)}}{T_s} = -\lambda \eta_1^2(0, t) + \eta_1^3(0, t) + \frac{1}{3} \eta_1(0, t) \eta_{1xx}(0_-, t) + \frac{1}{6} \eta_{1x}^2(0_-, t), \quad (28)$$

where $M_{hs}^{(1)}$ is the horizontal momentum of an upstream soliton. After adopting the following approximation,

$$\lim_{T \rightarrow \infty} \frac{1}{T} \int_0^T \eta_1(0, t) dt = h_s, \quad (29)$$

$$\lim_{T \rightarrow \infty} \frac{1}{T} \int_0^T \eta_1^2(0, t) dt = h_s^2, \quad (30)$$

$$\lim_{T \rightarrow \infty} \frac{1}{T} \int_0^T \eta_1^3(0, t) dt = h_s^3, \quad (31)$$

$$\lim_{T \rightarrow \infty} \frac{1}{T} \int_0^T \eta_1(0, t) \eta_{1xx}(0_-, t) dt = 0, \quad (32)$$

$$\lim_{T \rightarrow \infty} \frac{1}{T} \int_0^T \eta_{1x}^2(0_-, t) dt = 0, \quad (33)$$

the long time average of the above two first integrals becomes

$$\frac{m_s}{T_s} = -\lambda h_s + \frac{3}{4} h_s^2, \quad (34)$$

$$\frac{M_{hs}^{(1)}}{T_s} = -\lambda h_s^2 + h_s^3. \quad (35)$$

The operation (35)/(34) results in

$$a_s = \frac{2(h_d + \frac{4}{3}\lambda)(h_d + \frac{1}{3}\lambda)}{h_d}. \quad (36)$$

To find T_s , perform the operation $\int_{-\infty}^{x_D} (1) dx$ where x_D is any point in the uniform depression zone. This integral yields

$$T_s = \frac{16}{3} \left[\frac{2(h_d + \frac{1}{3}\lambda)}{3h_d^3(h_d + \frac{4}{3}\lambda)} \right]^{1/2}. \quad (37)$$

Acknowledgment

This work was supported in part by the Natural Sciences and Engineering Research Council of Canada.

References

- [1] S.J. Lee, G.T. Yates, and T.Y. Wu, "Experiments and analyses of upstream-advancing solitary waves generated by moving disturbances", *J. Fluid Mech.* 199, 569–593 (1989).
- [2] W.K. Melville and K.R. Helfrich, "Transcritical two-layer flow over topography", *J. Fluid. Mech.* 178, 31–52 (1987).
- [3] R.H.J. Grimshaw and N. Smyth, "Resonant flow of a stratified fluid over topography", *J. Fluid Mech.* 169, 429–464 (1986).
- [4] S.S.P. Shen, "Forced solitary waves and hydraulic falls in two-layer flows", *J. Fluid Mech.* 234, 583–612 (1992).
- [5] S.S.P. Shen, "Locally forced critical surface waves in channels of arbitrary cross sections", *J. Appl. Math. Phys. (ZAMP)* 42, 122–138 (1991).
- [6] T.Y. Wu, "Generation of upstream advancing solitons by moving disturbances", *J. Fluid Mech.* 184, 75–90 (1987).